

# Printing Angle Sensors for Foldable Robots

Xu Sun<sup>1</sup>, Samuel M. Felton<sup>2</sup>, Robert J. Wood<sup>2</sup>, and Sangbae Kim<sup>1</sup>

**Abstract**—Self-folding is a promising technique for assembling robots from flat sheets. However, existing implementations do not include reliable methods for sensing the folding angle, making feedback control impossible. In this paper, we present novel angle sensors for foldable robots and machines. They are inkjet printed and fully integrated into robots' laminate. This additional sensor layer tracks the angle motion of robot hinges, to better guide robot assembling by folding and to perform more complicated tasks that requires feedback control, making folded robots more capable in real world applications. We introduce the fabrication process, property assessments, and demonstrate sensor performance by measuring folding angles of a cube and controlling folds on a gripper.

## I. INTRODUCTION

Techniques to fabricate robots by folding have gained interest in the robotics field because they are inexpensive and can produce lightweight, complex geometries [1]. We refer to these techniques as 'printable manufacturing' because they can rapidly fabricate a machine from a digital blueprint using inexpensive tools such as laser cutters. A scaled Smart Composite Microstructure (SCM) process, for example, can produce a robot for less than one dollar and takes less than an hour to build [2]. Self-folding methods can make this fabrication technique even faster by enabling robots to self-assemble their 3D geometry. There are many existing self-folding methods including shape memory polymers [3], magnetics [4], [5], polymer swelling [6], and pneumatics [7]. However, in order to be a viable method for printable manufacturing, the self-folding technique must be robust, flexible, and inexpensive.

The accuracy of folding is a significant metric for self-folding performance, as it ultimately determines the final folded 3D geometry and affect the robot's functionality. In past experiments, researchers were able to achieve angle-controlled folds with mechanical stops [8] and by changing the self-folding hinge geometry [9]. However, these techniques resulted in a standard deviation of at least 5° [9]. This variation can result in incomplete and non-functional machines. This problem is exacerbated in the case of sequential self-folding, because errors will propagate from step to step. In the case of [9], the success rate of a robot's self-folding process is only about 30%.

One self-folding and actuation method utilizes printable pneumatic actuators called "pouch motors" to actively control the folding joints. In our previous work, we developed

a model which predicted fold angle based on readings of pouch pressure [7], allowing for some open loop control. However, that pressure control system was only accurate if the load on the hinge was negligible. In particular, the fold angle was significantly affected by gravity, which the open loop model did not account for. In addition, these same self-folding hinges may be used as the dynamic component of these machines. Since the hinges will be undergoing some load for many of their applications [10], a direct position reading of the fold angle is desirable.

A variety of sensors capable of measuring a folded angle have been developed, but most rely on discrete components or expensive and time-consuming techniques, making them incompatible with a printable process. Many discrete components have been used for measuring joint angles in robotics systems, including magnetic and rotary encoders [11], [12], accelerometers, and gyroscopes [13]. Soft sensors have been used to measure the angle of self-folding shape memory alloy hinges, but each sensor and hinge must be installed individually [14]. Carbon based piezoresistive sensors can also be used to measure folding angles. They can be fabricated by screen printing [15] or pencil drawing [16]. Because these processes are manual, we found their quality to be inconsistent, limiting their performances. In contrast, fabrication by printing is a reliable automated process that has already been used to make electrical components such as circuits [17], batteries [18], optics [19], and polymer transistors [20]. In particular, we found the working principle behind piezoresistive sensors a promising method for angle sensing: when folded, the distances between carbon particles deposited on the substrate vary. This results in a resistance change proportional to the angular displacement at the fold. Therefore, we explored the automated printing solution to make piezoresistive sensors.

In this paper, we present a printable self-folding hinge that includes embedded angular sensors for feedback control. We print conductive ink onto the self-folding composite to produce piezoresistive angle sensors along the self-folding hinges. We describe the design and fabrication process of making and embedding the sensor layer into a folded robot's structure. Then we assess the quality of printed piezoresistive sensors and their performance in angle measurements. We demonstrate robotic applications of such hinges on a cubic structure and a gripper, and discuss other impacts and future work.

<sup>1</sup>X. Sun and S. Kim are with Department of Mechanical Engineering, Massachusetts Institute of Technology, 77 Massachusetts Avenue, Cambridge MA, USA. xusun@mit.edu

<sup>2</sup>S. M. Felton and R. J. Wood are with the School of Engineering and Applied Sciences and the Wyss Institute for Biologically Inspired Engineering, Harvard University, Cambridge, MA, USA.

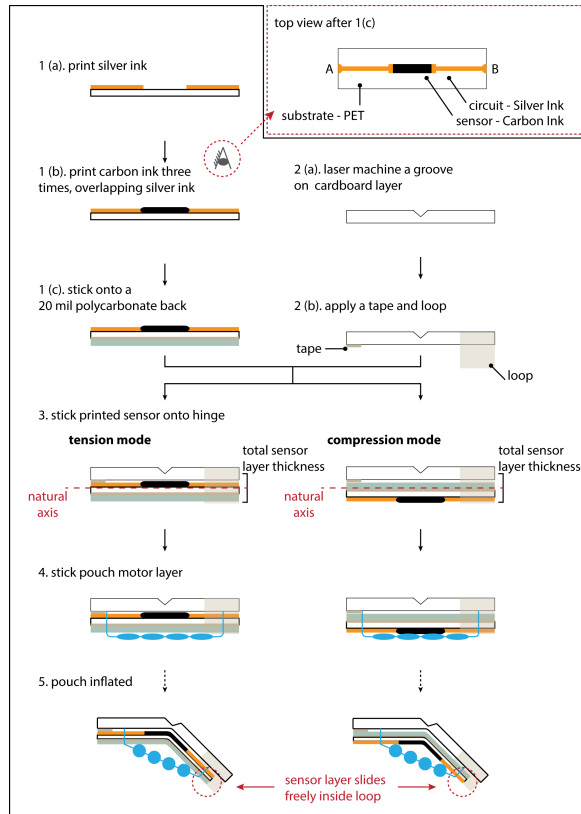


Fig. 1. Fabrication process of a simple foldable hinge and embedded printed angle sensor

## II. DESIGN AND FABRICATION

### A. Basic Design of a Hinge with Sensor Layer

The sensor layer presented here is compatible with a variety of laminate designs such as those used to make several folded robots [2], [3], [7]–[9], [21]. It can be quickly and easily reproduced with off-the-shelf products. In this paper, we focus on fabricating it on pneumatic self-folding structures [7] because it demonstrates a feedback control capability that this sensor layer can add.

### B. Materials and Fabrication

Fig. 1 shows the complete fabrication process of a foldable hinge integrated with printed sensor layer and pouch motor layer. The sensor is directly printed with a piezoelectric inkjet printer. It deposits carbon resistive ink for the sensing part and silver nano-particle ink for the terminals and connecting circuits. In order to achieve high printing quality, it is important to optimize ink viscosity, density, surface tension and particle size [17]. We choose the Methode 3804 resistive carbon nano particle ink to make the sensing part. It is \$200 per bottle of 100 ml, which is equivalent to \$0.02 per sensor we make. We choose Mitsubishi NBSIJ-MU01 silver nano particle ink to make the circuitry part. It is \$340 per bottle of 100 ml, which is equivalent to \$0.48 per meter of 1mm trace.

The silver ink only sinters on glossy photo paper and PET films, while the carbon ink sinters on substrates including

polyester, acrylic and synthetic polymer sheets. In our case, we choose a transparent PET film product from Mitsubishi Imaging (item number NB3GUA4X100) as the substrate. This material provides a little additional spring back force to the hinge, which helps a folded hinge to reflect back to flat if desired.

Although any commercially available piezoelectric printers can be used to deposit carbon and silver ink, we choose Brother DCP-J152W printer, because this printer deposits more amount of ink per unit area, resulting in better sensor quality with carbon ink and lowering circuitry resistivity with silver ink. Kawahara et al. have provided a guideline of silver ink printing settings [17]. Because in our case, we loaded silver ink in all color cartridges but carbon ink only in black cartridges, the table below shows our modified printing settings.

TABLE I  
PRINTER SETTINGS

	Print Silver ink	Print Carbon ink
Media Type	Other photo paper	Plain paper
Print Quality	Best	Best
Color Mode	Vivid	N/A
Color/ GreyScale	Color	Grey scale
Color Enhancement	checked	checked
Color Density	+2	N/A
Improved Pattern Printing	Checked	Checked

Because both silver and carbon particles are bigger than normal inkjet ink particle, even with the optimized setting, printing silver and carbon particles still cause clogging more often than regular inkjet inks, resulting in broken lines and therefore nonfunctional circuits. In order to achieve repeatable consistent quality, it is necessary to clean the printhead using printer's built-in function regularly.

The circuitry part is first printed using settings shown in column 1 of table 1. Then the sensor part is printed using settings shown in column 2. The sensor part is repeatedly printed three times to make sure the sensor pattern is completely filled with carbon ink, which greatly reduces noise in readings.

Generally, larger radius of curvature helps to produce wider range of readings. In most applications, we adhered the printed PET onto a 20 mil polycarbonate film. It gives the sensor an additional stiffness and makes the radius of curvature larger. It also provides an additional spring back force when bended, allowing the hinge to unfold when the pressure is relieved.

One end of the sensor is taped down onto the structure layer. The other end is left to slide freely in a strapped loop. It can be taped either with the ink surface facing the cardboard, or with the polycarbonate back facing the cardboard. We call the first scenario the tension mode: during bending, the ink layer is above the natural axis and experiences tension. Printed carbon particles are pulled apart raising sensor resistance. We call the second scenario the compression mode: during bending, the ink layer is below the natural axis and

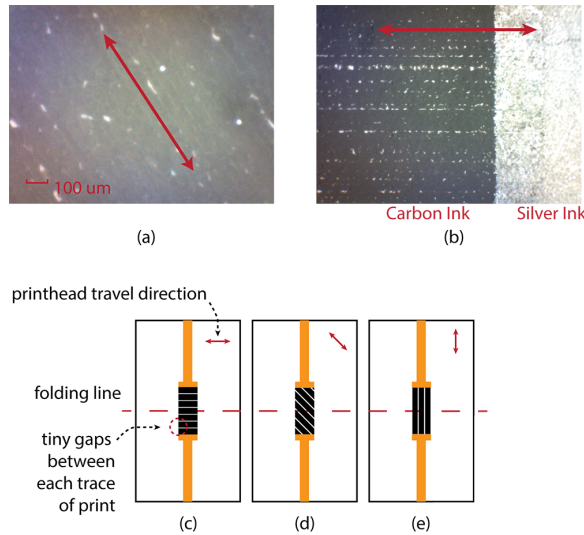


Fig. 2. Print head travel direction and gaps between each trace are observed. (a) a closer look at the sensor part, white dots are unprinted gaps (b) comparing print quality of carbon ink and silver ink (c), (d) and (e) illustrate the samples for quality testing. Their print head travel direction and gaps orientated differently with respect to folding line

experiences compression. Printed carbon particles are been pushed closer, reducing the sensor resistance. This property makes the sensor bi-directional. Over the experiments, we found that the tension readings appears to be smoother with a larger readable range. We used the tension readings for the rest of the paper.

For pneumatic self-folding machines, a pouch motor layer is included. It is fabricated with a thermal drawing process [22], and attached to the hinge. When inflated, the pouch contracts lengthwise, pulling the two faces together and causing the hinge to fold. When it is deflated, sensor layer provides a spring back force, re-straightening the fold.

### C. Fabrication Quality

In theory, the width and length of the sensor design determines its resistance. The carbon ink we used has a sheet resistance of  $R_s = 5k\Omega/\square$

$$R = R_s \frac{L}{W} \quad (1)$$

In reality, this method does not work well, because consumer level piezo-electric printer produces random gaps between traces of each print head travel. To evaluate printed sensor quality, we used an optical microscope to observe the sensor.

We observed that the carbon ink appeared much smoother than the silver ink. We also found the random gaps introduce higher resistivity especially when it is oriented parallel to the fold, impeding fabrication repeatability and versatility. To closer examine this effect, we prepared 3 groups of 10 samples, each has the random gaps parallel to traces of print and oriented differently with respect to the folding line: 10 are oriented  $0^\circ$  (Fig. 2c), 10 are oriented  $45^\circ$  (Fig. 2d) and 10 are oriented  $90^\circ$  (Fig. 2e). We measured th resistance of

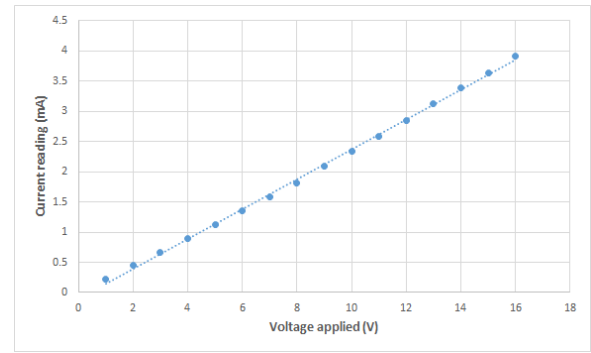


Fig. 3. Electrical property of the printed sensor

each sensor at the unfolded state and at  $90^\circ$  folded state. We found that:

- Within one group, the resistance of each sample varies. The group shown in Fig. 2c has the greatest standard deviation of  $9.8^\circ$ . We believe this is due to the minor clogging developed on the print head over the printing process. The thickness of the deposited ink therefore becomes thinner over time.
- The average resistances of each group varies. This is because the gaps between a carbon particle to its adjacent particle deposited within one print head travel (1 trace of print) is smaller than that to the adjacent trace.
- The percentage change in resistance between the unfolded state and a  $90^\circ$  folded state is consistent across all groups, with a standard deviation of 2.2%. This indicates the slope of resistance to angle plot to be consistent, and further indicates that they are suitable for angular displacement measurements.

In conclusion, because sensors do not have very consistent quality from printing, the resistance of a newly printed sensor always needs to be measured. The change in resistance per change in angle for sensors with the same printed geometry are consistent. For the best quality, print orientation shown in Fig. 2e are used to produce single printed sensors.

## III. SENSOR PROPERTIES AND PERFORMANCE EVALUATION

### A. Electrical Properties

We measured the current passing through an unfolded 4.5mm by 20mm printed sensor when supplied with a range of voltages to see if the resistance varies under different electrical loads. Figure 3 shows the resulting current as a function of voltage, indicating ohmic behavior over the range of 0-16V.

### B. Angle Reading Test setup

We made a testing fixture with a potentiometer and a servo motor. The potentiometer is attached to the axis of rotation of a hinge. The servo motor can turn the right tab to rotate counter clockwise, as shown in Fig. 4a. We fixed the testing sample on top of the left tab. As the right tab rotates, it

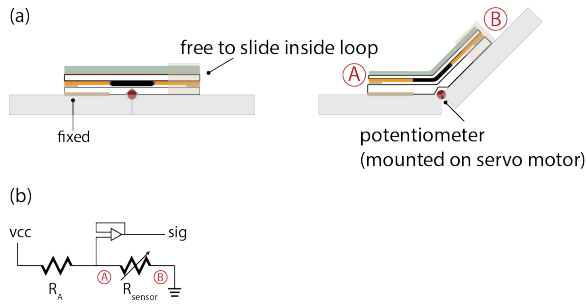


Fig. 4. Testing hardware setup (a) shows the side view of the setup. The hinge is flipped and mounted onto the fixture. (b) circuit drawing of the setup

pushes up the right end of the cardboard hinge, causing it to fold.

A sensor sample is connected in the circuit in Fig. 4b.  $R_A$  acts like a voltage divider. Its value is set to be equal to the resting resistance of the printed sensor. Every few seconds, servo motor turns to a “true” angle, causing the printed sensor layer to bend and bring up the value of  $R_{sensor}$ . This results in a change in voltage and is read by a microprocessor.

### C. Angle Reading Test: folding at different speeds

To filter out noise, for every angle we measure, we take 10 readings at a time and average them. From previous experiments, we observed readings take a little time to settle after the immediate change in angle. This may attribute to the viscoelastic behavior of the sensor film. To obtain more accurate data, for each trial, we coded our program to wait a few seconds ( $t_{wait}$ ) before a new reading is taken. We run ten trials with three different angular velocities (by changing  $t_{wait}$  from 25ms delay, to 200ms delay and then to 3000ms delay) to determine if the folding rate effects the sensor output.

Fig. 5 shows the angle of the hinge as measured by our printable sensors. In these three plotted trials, the servo motor turns the hinge at 5.9°/s, 3.2°/s, and 0.4°/s. From this figure, we can observe a linear relationship of the sensor reading with respect to command angle. The mean of the standard deviation across all time points for each velocity were 2°, 1°, and 2°, degrees respectively.

The data also indicates that the speed of the hinge rotation has little effect on the sensor’s output or its precision, although at the very beginning of the motion there does seem to be a relative increase in the sensor output at high speeds. This effect appears to drop off after 15°, and may be related either to acceleration of the hinge, or its geometry in the flat state.

### D. Angle Reading Test: Repeatability

To further investigate how well the sensor can produce the same reading repeatably at the same folded position, we commanded the sensor to fold to a 30° angle from unfolded state (0° folding angle) 30 times (Fig. 6). In each case the hinge is folded as quickly as possible, and the final angle is reached in less than 0.5s.

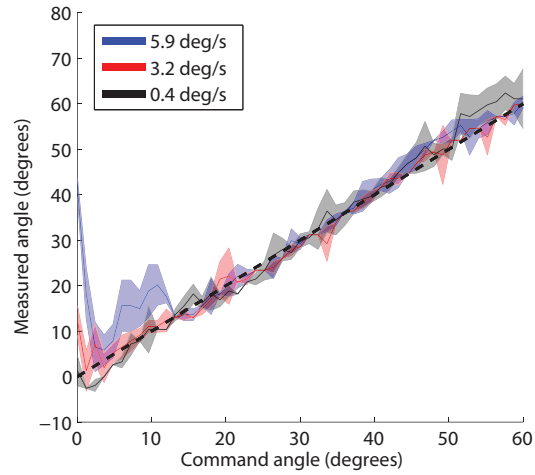


Fig. 5. Measured angle as a function of command angle at three different speeds: 5.9°/s, 3.2°/s, and 0.4°/s. The shaded region indicates standard deviation, N=4. The dashed line indicates the true angle.

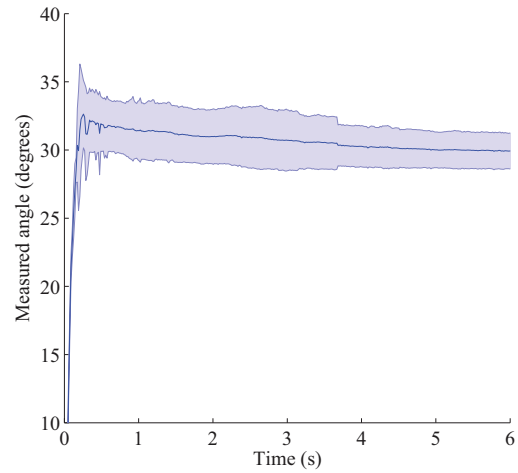


Fig. 6. Measured angle of a hinge upon near instantaneous (<0.5 s) folding to 30°. The shaded region indicates the standard deviation, N=30.

We found that the sensor reading drops slowly over time. This may attribute to the stress relaxation behavior of the material. The standard deviation of the angular measurement is 2° one second after folding. This is much higher when the sensor is first folded; this may be due to the sensor ‘settling’ in some way, or may be variance in the speed at which the final angle was reached.

### E. Angle Reading Test: Sensor Width Influence

We noticed that the width of the sensor also impact the angle reading accuracy. To better understand this behavior, using the same hardware setup and folding procedure, we evaluated 4 sensor samples with width 2mm, 4mm, 8mm and 16mm, all of which are 12mm long.

As shown in Fig. 7, we found that as width increases from 2mm to 8mm, the standard deviation decreases. 16mm sensor had the same performance as the 8mm sensor. This may be

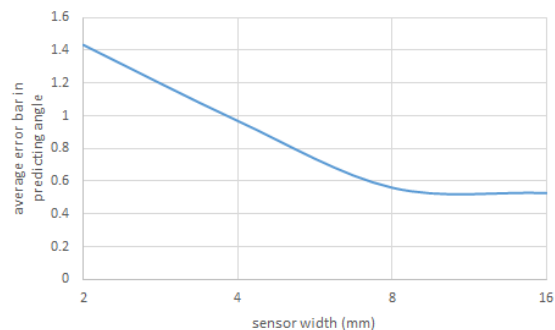


Fig. 7. Effect on angle reading accuracy from sensor width

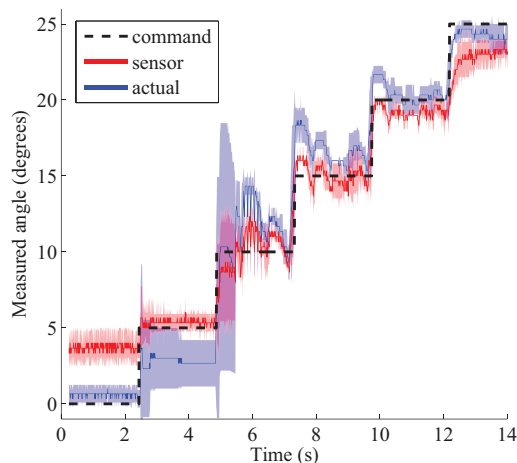


Fig. 8. Command signal (dashed), printed sensor reading (red) and actual angle (blue) of the hinge. The actual angle is measured by a potentiometer attached to the hinge. Shaded region indicates standard deviation,  $N=3$

because as width increases and more ink are deposited, more randomness of gaps and uneven thickness are also introduced with the inaccurate printing process.

To validate this sensor as a method for angular control, we built a hinge and designed a bang-bang control system. In this system, a pressure and a release valve are installed in series with the pouch motor. When the sensor signal drops more than a degree below the command signal, the pressure valve opens. Conversely, when the sensor signal is greater than the command signal by a degree, the release valve opens. Our pneumatic system also leaks, resulting in a slow decrease in angle over time. However, this behavior seems to be insignificant for the time frame of our experiments.

The command signal consists of a series of  $5^\circ$  steps from  $0^\circ$  to  $25^\circ$ . The angle measured by the printed sensor is plotted as a function of time in Fig. 8, along with the command signal and actual hinge angle as measured by a potentiometer. Since the hinge is pneumatically controlled by refilling and releasing pressure, after receiving a new commanded angle, both actual angle reading and sensor angle readings fluctuate and gradually approaching the commanded. From  $15^\circ$  to  $25^\circ$  the hinge responds appropriately to the commands, staying within  $2^\circ$  of the input angle after settling at each step. At

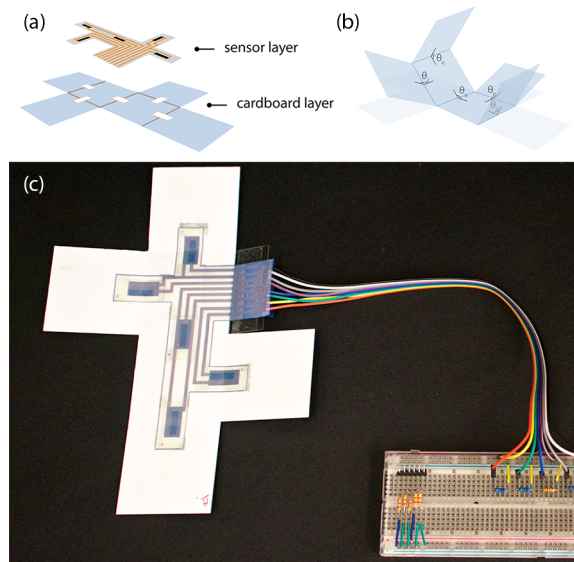


Fig. 9. (a) sensor layer embedded in an unfolded cube (b) shows the angles it tracks (c) final cube model

lower angles at the beginning of the test, the sensor reading exhibits larger errors, which may be a result of the geometry of the hinge approaching the singularity of a flat state.

#### IV. APPLICATIONS

##### A. Track Cube Folding

To demonstrate how the sensor can be used to track foldings, we laser machined a piece of cardboard that is ready to be folded into a cube, and embedded it with a sensor layer that can monitor folding angles of all hinges, as shown in Fig. 9.

We first calibrated each sensor by recording the reading at the unfolded state ( $0^\circ$  folding angle) and the reading at  $90^\circ$  folded state, and assuming a linear relationship between those two points according to our performance evaluation result. In the demonstration, the microprocessor collects 40 readings after a 2.5-seconds delay per 3 seconds period. It maps the shape of the folded cube and illustrates it (see Supp. Video).

In this demonstration, the sensor successfully tracks angles below  $90^\circ$  with an error of about  $5^\circ$ . The long time gap between each new data output is necessary to reduce stress relaxation effect and filter out some noise.

##### B. Controlling a gripper

To demonstrate how the sensor can be used in a robotic structure to provide feedback loop control, we made a gripper with five fingers actuated by pouch motors, as shown in Fig. 10. Although each finger has two joints, this gripper has a single input because the pouch motors are linked to a single source. Five angle sensors are printed in a network and mounted on the opposite face of the gripper. These five sensors only monitor the folding angles of knuckle joints. Because each joint has the same geometry and pressure, we expect each joint to have the same angle. Therefore, we take

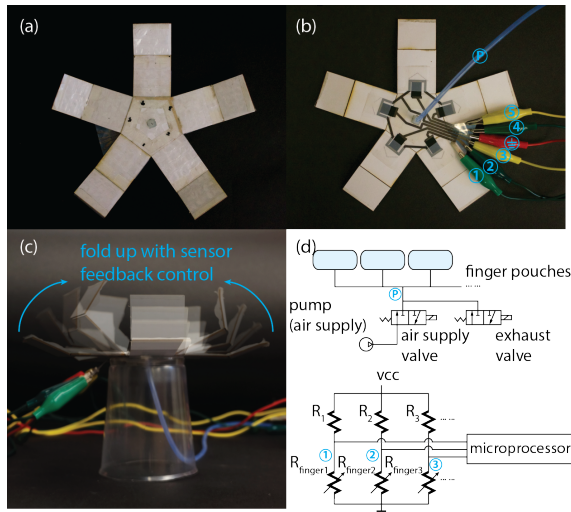


Fig. 10. (a) gripper top view: pouch motor layer; (b) gripper bottom view: sensor layer. The connection are marked corresponding to the control circuits in (d); (c) gripper folding in action; (d) shows the pneumatic and circuits control

an average of all five readings and only use the average to determine to final fold. This way, we are able to reduce the data output time by 80% compared to early cases.

We calibrated sensors using the same method in the cube demonstration. During demonstration, we used two valves to regulate air inside the pouch. Both valves are closed at the desired folding angle. If the folding angle is  $4^\circ$  bigger or smaller than the desired folding angle, the valves either opens the pouch to the air to exhaust some pressure or connect the pouch to a pump to refill air. We successfully commanded the fingers to fold to different openness with the sensors.

In order to better illustrate position feedback, at the  $60^\circ$  folding angle, we forced open the gripper by hand, and felt immediate response that it tries to push back. Once the hand is moved away, the gripper adjusts back to its commanded position. The fingers appeared to fold the same as before the intervention.

## V. DISCUSSION

We introduced a novel printable piezoresistive sensor well-suited for folded robots. We described the simple fabrication process and tested a variety of sensor properties. This sensor changes resistance linearly with respect to folded angle and is highly reliable over time. However, when taking angle readings, it has a short delay of about 0.5 s and has an error of about  $2^\circ$ .

With two demonstrations on a cube and a gripper, we showed that this printed sensor can be readily embedded into folded robots to track folding motions and provide a position feedback control. We used a bang-bang controller in these experiments due to hardware limitations; the valves in our system had only 'open' and 'closed' states. However, these sensors are compatible with continuous feedback control methods. We believe this printable sensor to be a useful toolkit for future folded robot developments to help

them self-assemble more accurately and perform controllable tasks.

It is also important to note that the linear relationship between the sensor output and folding angles are based on our repeated observations. Further works with a more thorough model could reveal a more complicated relationship.

We have yet to study any long-term drift of the sensors. Preliminary observations indicate that sensors' resting resistance can drift substantially before settling after two days. We believe this is due to evaporation of some components of the conductive ink, but further investigation is required.

Currently each sensor must be calibrated independently. In addition, multiple measurements must be taken and averaged, slowing down the sensing frequency. We believe this variance can be improved through better mechanical design, a more reliable printing process, and better characterization.

## ACKNOWLEDGMENT

We appreciate the help and guidance from Meng Yee (Michael) Chuah. This project is supported by National Science Foundation (Grant number: EFRI-1240383 and CCF-1138967).

## REFERENCES

- [1] C. D. Onal, M. T. Tolley, R. J. Wood, and D. Rus, "Origami-inspired printed robots."
- [2] A. M. Hoover and R. S. Fearing, "Fast scale prototyping for folded millirobots," in *Robotics and Automation, 2008. ICRA 2008. IEEE International Conference on*. Ieee, 2008, pp. 886–892.
- [3] Y. Liu, J. K. Boyles, J. Genzer, and M. D. Dickey, "Self-folding of polymer sheets using local light absorption," *Soft Matter*, vol. 8, no. 6, pp. 1764–1769, 2012.
- [4] J. W. Judy and R. S. Muller, "Magnetically actuated, addressable microstructures," *Journal of Microelectromechanical Systems*, vol. 6, no. 3, pp. 249–256, 1997.
- [5] M. Boncheva, S. A. Andreev, L. Mahadevan, A. Winkleman, D. R. Reichman, M. G. Prentiss, S. Whitesides, and G. M. Whitesides, "Magnetic self-assembly of three-dimensional surfaces from planar sheets," *Proceedings of the National Academy of Sciences of the United States of America*, vol. 102, no. 11, pp. 3924–3929, 2005.
- [6] J. Guan, H. He, D. J. Hansford, and L. J. Lee, "Self-folding of three-dimensional hydrogel microstructures," *The Journal of Physical Chemistry B*, vol. 109, no. 49, pp. 23 134–23 137, 2005.
- [7] X. Sun, S. M. Felton, R. Niiyama, R. J. Wood, and S. Kim, "Self-folding and self-actuating robots: A pneumatic approach," in *Robotics and Automation (ICRA), 2015 IEEE International Conference on*. IEEE, 2015, pp. 3160–3165.
- [8] S. M. Felton, M. T. Tolley, C. D. Onal, D. Rus, and R. J. Wood, "Robot self-assembly by folding: A printed inchworm robot," in *2013 IEEE International Conference on Robotics and Automation (ICRA)*. IEEE, 2013, pp. 277–282.
- [9] S. Felton, M. Tolley, E. Demaine, D. Rus, and R. Wood, "A method for building self-folding machines," *Science*, vol. 345, no. 6197, pp. 644–646, 2014.
- [10] R. Niiyama, D. Rus, and S. Kim, "Pouch motors: Printable/inflatable soft actuators for robotics," in *2014 IEEE International Conference on Robotics and Automation (ICRA)*, 2014.
- [11] Y. Kikuchi, F. Nakamura, H. Wakiwaka, and H. Yamada, "Index phase output characteristics of magnetic rotary encoder using a magneto-resistive element," *Magnetics, IEEE Transactions on*, vol. 33, no. 5, pp. 3370–3372, 1997.
- [12] T. Kojima, Y. Kikuchi, S. Seki, and H. Wakiwaka, "Study on high accuracy optical encoder with 30 bits," in *Advanced Motion Control, 2004. AMC'04. The 8th IEEE International Workshop on*. IEEE, 2004, pp. 493–498.
- [13] P. Cheng and B. Oelmann, "Joint-angle measurement using accelerometers and gyroscopes survey," *Instrumentation and Measurement, IEEE Transactions on*, vol. 59, no. 2, pp. 404–414, 2010.

- [14] J. K. Paik, R. K. Kramer, and R. J. Wood, "Stretchable circuits and sensors for robotic origami," in *Intelligent Robots and Systems (IROS), 2011 IEEE/RSJ International Conference on*. IEEE, 2011, pp. 414–420.
- [15] X. Liu, M. Mwangi, X. Li, M. O'Brien, and G. M. Whitesides, "Paper-based piezoresistive mems sensors," *Lab on a Chip*, vol. 11, no. 13, pp. 2189–2196, 2011.
- [16] C.-W. Lin, Z. Zhao, J. Kim, and J. Huang, "Pencil drawn strain gauges and chemiresistors on paper," *Scientific reports*, vol. 4, 2014.
- [17] Y. Kawahara, S. Hodges, B. S. Cook, C. Zhang, and G. D. Abowd, "Instant inkjet circuits: lab-based inkjet printing to support rapid prototyping of ubicomp devices," in *Proceedings of the 2013 ACM international joint conference on Pervasive and ubiquitous computing*. ACM, 2013, pp. 363–372.
- [18] K. Sun, T.-S. Wei, B. Y. Ahn, J. Y. Seo, S. J. Dillon, and J. A. Lewis, "3d printing of interdigitated li-ion microbattery architectures," *Advanced Materials*, vol. 25, no. 33, pp. 4539–4543, 2013.
- [19] K. Willis, E. Brockmeyer, S. Hudson, and I. Poupyrev, "Printed optics: 3d printing of embedded optical elements for interactive devices," in *Proceedings of the 25th annual ACM symposium on User interface software and technology*. ACM, 2012, pp. 589–598.
- [20] H. Sirringhaus, T. Kawase, R. Friend, T. Shimoda, M. Inbasekaran, W. Wu, and E. Woo, "High-resolution inkjet printing of all-polymer transistor circuits," *Science*, vol. 290, no. 5499, pp. 2123–2126, 2000.
- [21] E. Hawkes, B. An, N. Benbernou, H. Tanaka, S. Kim, E. Demaine, D. Rus, and R. Wood, "Programmable matter by folding," *Proceedings of the National Academy of Sciences of the United States of America*, vol. 107, no. 28, pp. 12 441–12 445, 2010.
- [22] R. Niiyama, X. Sun, C. Sung, B. An, D. Rus, and S. Kim, "Pouch motors: Printable soft actuators integrated with computational design," *Soft Robotics*, to appear.